Microscopic study of the magnetic coupling in a nanocrystalline soft magnet

1999 J. Phys.: Condens. Matter 11 2841

(http://iopscience.iop.org/0953-8984/11/13/018)

J. Phys.: Condens. Matter **11** (1999) 2841–2847. Printed in the UK PII: S0953-8984(99)98768-4

Microscopic study of the magnetic coupling in a nanocrystalline soft magnet

T Kemény†, D Kaptás†, J Balogh†, L F Kiss†, T Pusztai†‡ and I Vincze†‡

† Research Institute for Solid State Physics and Optics, H-1525 Budapest, PO Box 49, Hungary
‡ Department of Solid State Physics, Eötvös University, Budapest, Hungary

Received 28 October 1998

Abstract. The magnetic behaviour of nanosize ferromagnetic bcc granules embedded in an amorphous tissue (i.e., partially crystallized $Fe_{80}Zr_7B_{12}Cu$ amorphous alloy) was studied by ^{57}Fe Mössbauer spectroscopy. The results are compared with the bulk counterparts: bcc-Fe and amorphous $Fe_2B_{0.625}Zr_{0.375}$. Size dependent enhancement of the Curie point of the nanosize amorphous phase was not observed. At temperatures well above the Curie point of the amorphous phase superparamagnetic relaxation of the bcc crystallites is observed opening new possibilities to study the anisotropy energy of nanosize ferromagnetic grains.

1. Introduction

Recently very good soft magnetic materials with high initial magnetic permeability and low coercitivity have been found [1]. The nanocrystalline Fe–Cu–Nb–Si–B (i.e., Finemet) and Fe–Zr–B–Cu alloys [1, 2] belong to this class of materials. These nanocrystalline alloys are prepared by partial crystallization of amorphous ribbons resulting in nanosize crystalline bcc precipitates in a residual amorphous matrix. It is often assumed [1, 3] that magnetic properties are seriously influenced by magnetic exchange interactions between the adjacent ferromagnetic grains mediated by the intergranular amorphous matrix. The hypothesis of strong exchange coupling via the amorphous spacers would involve two consequences: an enhancement and a considerable smearing out of the Curie temperature. The smearing out can also be a result of concentration fluctuations. Magnetic measurements reported [4] an increase of the Curie temperature of the intergranular amorphous region in nanocrystalline alloys of the order of 100 K. On the other hand, a recent ^{57}Fe Mössbauer spectroscopy (MS) study of a low B content nanocrystalline Fe–Zr–B–Cu alloy did not find [5] any appreciable smearing out of the Curie temperature of the amorphous interphase beyond the effect of the stray magnetic field of the ferromagnetic bcc granules. The present work is aimed at investigating the magnetic coupling of granular materials by a local probe, i.e., by ^{57}Fe MS. Nanocrystalline $Fe_{80}Zr_7B_{12}Cu$ is selected for this purpose, where the bulk counterpart of the residual amorphous phase was also successfully prepared. The MS measurements were performed between 12 K and 900 K in a closed cycle (APD) cryostat and a home-made vacuum furnace.

The composition dependence of the hyperfine field, isomer shift and Curie temperature in the amorphous $Fe_2(B_{1-x}Zr_x)$ system will be reported separately [6]. This work uses only the results for $Fe_2B_{0.625}Zr_{0.375}$. The nanocrystalline sample, nc-$Fe_{80}Zr_7B_{12}Cu$, was produced by a heat treatment at 900 K, i.e., after the first crystallization stage of the amorphous ribbon of the above composition, which was melt spun in a protective atmosphere. The nanocrystalline

0953-8984/99/132841+07$19.50

state of the alloy was checked by x-ray diffraction using Cu Kα radiation and Bragg–Brentano geometry. The results were evaluated in two ways. The Rietveld full profile matching technique was applied using the program FULLPROF. The additional line broadening observed for the nanocrystalline sample (i.e., that beyond the instrumental resolution, determined by a standard Si sample) was assigned to the effect of crystallite sizes, D and microstrains, resulting in $D = 10 \pm 2$ nm. Second, a standard Williamson–Hall plot (i.e., the excess line width, FWHM* sin(Θ) versus cos(Θ) plot) was used. Here the best fit line intercepts the ordinate at $k^*\lambda$/(size) where k is the Scherrer constant (0.9) and λ is the x-ray wavelength (1.54 Å). The crystallite size derived this way is 8 ± 2.5 nm, in agreement with the previous result.

The MS results [7–10] on Fe–Zr–B–Cu nanocrystals are controversial concerning the structure of the nanocrystalline bcc phase and the interfacial zones. The shoulder of the bcc-Fe lines (marked as B_s below) is often attributed to an interfacial phase. These issues are also closely related to the estimation of the composition of the residual amorphous phase. As this is based on the determination of the spectral ratio of the bcc phase, it is essentially changed when a part of the spectrum is attributed to an interfacial zone. This is especially important when comparison of Curie points is made since small changes in the concentration can cause large variation of T_C.

Mössbauer spectra of nc-$Fe_{80}Zr_7B_{12}Cu$ and a-$Fe_2B_{0.625}Zr_{0.375}$ measured at 12 K are shown in figures 1(a) and (b), respectively. Two characteristic features can be distinguished in the nanocrystalline spectrum: a narrow sextet with asymmetric lines which will be attributed to the bcc granules and a broad magnetic component belonging to the residual amorphous phase. The stress between the precipitated bcc grains and the residual amorphous phase causes via magnetostriction a preferred orientation of magnetization. This magnetic texture is perpendicular to the ribbon plane (parallel to the gamma ray beam) and results in the suppression of the intensities of the 2–5 lines of the Mössbauer spectrum of figure 1(a).

The Mössbauer parameters (isomer shift, IS_m and hyperfine field, B_m) of the stronger component of the asymmetric sextet, which will be referred to as the main line, are similar to those of pure bcc-Fe at low temperature. The main line has a shoulder on the low field side which is quite broad; its hyperfine field is B_s. This shoulder structure is invariably observed when the nanocrystalline system contains early transition metals (Ti, V, Cr, Zr, Nb etc). A similar shoulder structure is observed [11] in the melt-quenched microcrystalline Fe–Zr solid solution. On the other hand, thin film studies [12] found no trace of this satellite in Fe/B multilayers even when the bcc Fe thickness is reduced below 3 nm, ruling out its interfacial origin.

With increasing temperature B_m decreases faster than the hyperfine field of pure bcc-Fe as shown in figure 2. B_s follows closely the temperature dependence of B_m in a broad temperature range as shown in the inset. Similar temperature behaviour is observed [11] in the melt-quenched microcrystalline Fe–Zr solid solution confirming that impurity effects are their common origin. It is thus obvious to assume that the nanocrystalline Fe-based bcc phase contains a few percentage of dissolved Zr and B. In this case B_m is the hyperfine field of Fe atoms with no Zr or B nearest and next nearest neighbours and B_s is the average hyperfine field of Fe atoms with at least one impurity neighbour in the first two coordination shells of this solid solution. This assignment is supported by the temperature dependence of B_m which indicates a Curie temperature of approximately 930 K, about 100 K lower than that of pure α-Fe. Magnetic measurements also indicate [13] lower Curie temperature for the nanocrystalline bcc phase than that of α-Fe. The total impurity content of this nanocrystalline bcc phase can be estimated from the relative intensities of the main line (0.35) and the satellite (0.18) in the Mössbauer spectra. Assuming random distribution of the Zr and B impurities the binomial formula yields less than 4 at.% for this impurity content.

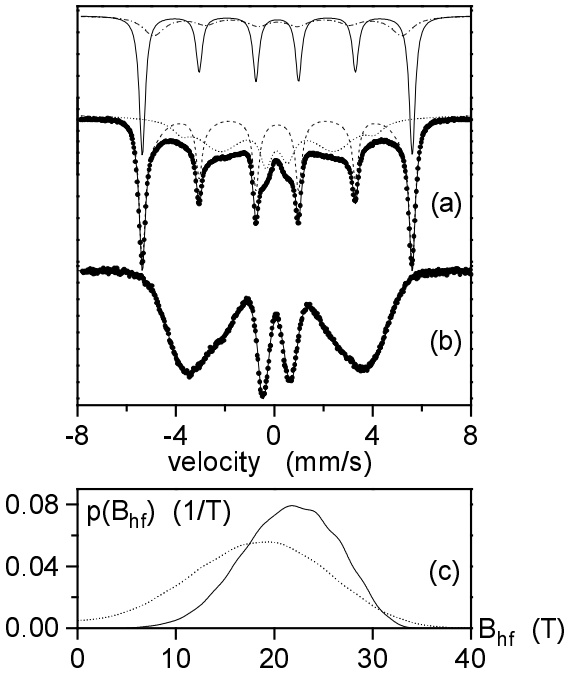

Figure 1. Mössbauer spectra of nc-$Fe_{80}Zr_7B_{12}Cu$ (a) and a-$Fe_2B_{0.625}Zr_{0.375}$ (b), taken at 12 K. The full lines are the fitted curves, in (a) the bcc nanocrystalline component (broken line) and the residual amorphous part (dotted line) are marked, respectively. The bcc component has two contributions as shown in the upper part of the figure: the main lines (continuous curve) and the satellite, i.e., the shoulder lines (dash–dot curve) are shown. In (c) the respective hyperfine field distributions are shown (a-$Fe_2B_{0.625}Zr_{0.375}$ (continuous line); residual amorphous phase of nc-$Fe_{80}Zr_7B_{12}Cu$ (dotted line)).

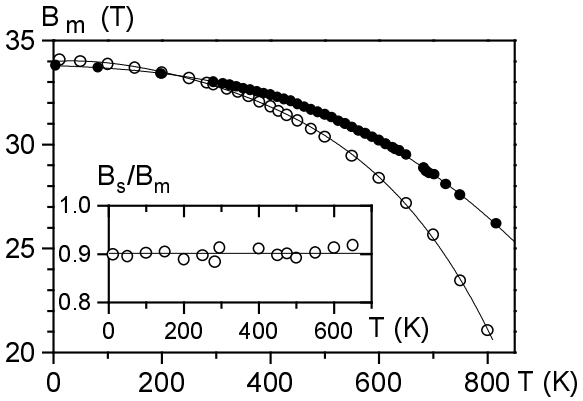

Figure 2. Temperature dependence of the hyperfine field of the main bcc component (open circles) in nc-$Fe_{80}Zr_7B_{12}Cu$ compared to that of pure α-Fe (filled circles). The inset shows the B_s/B_m (satellite to main line) ratio as a function of temperature.

The sum of these two components is the total relative number of Fe atoms in the bcc phase ($\alpha = 0.53$) which allows an estimation of the iron content of the residual amorphous phase.

The small amount of Cu (1 at.%), whose main role is triggering the nanocrystal formation by precipitating in a separate fcc phase [14], will be neglected. A simple material balance gives then the Fe concentration of the residual amorphous phase. This is 65 at.% Fe when the impurity content of the bcc phase is neglected and 69 at.% Fe when the 4 at.% Zr/B upper impurity content is taken into account, respectively. If the starting Zr to B ratio remains unchanged, the average composition of the residual amorphous matrix is approximated as $Fe_2B_{0.632}Zr_{0.368}$.

The characteristic size, d, of the amorphous granules can be estimated as [4] $d = D(p^{-1/3} - 1)$. It gives $d = 3$ nm with the $D = 10$ nm grain size and with the $p = 0.45$ atomic crystalline fraction (used as volume fraction, neglecting density differences) which is calculated from the $\alpha = 0.53$ bcc fraction of iron.

The residual amorphous phase is characterized by a hyperfine field distribution (dotted line in figure 1(c)), its average hyperfine field, B_a is 18 T. The average value of the isomer shift is $-0.047(14)$ mm s^{-1} (with respect to α-Fe). These values compare reasonably well to those of the $Fe_2B_{0.625}Zr_{0.375}$ amorphous ribbon. Its average isomer shift is $-0.035(12)$ mm s^{-1} reflecting rather similar Zr and B environments. The hyperfine field distribution—solid line in figure 1(c)—is narrower for the bulk amorphous phase and its average value, 21.6 T is slightly larger as compared to the nano-phase. These differences can be explained by composition fluctuations in the residual amorphous phase and slight deviations from the supposed average composition.

Determination of the Curie temperature of the bulk amorphous phase is quite straightforward. In the paramagnetic state at high temperatures the Mössbauer spectrum consists of a well defined quadrupole splitted line. Below the Curie temperature (396 ± 1 K) the apparent value of this average quadrupole splitting, ΔE_Q, increases considerably (empty circles in figure 3) thus characterizing a sharp transition.

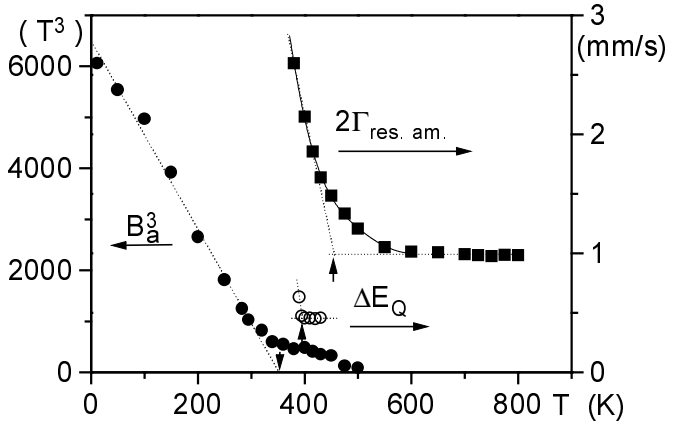

Figure 3. Mössbauer determination of the Curie temperatures of a-$Fe_2B_{0.625}Zr_{0.375}$ and the residual amorphous phase of nc-$Fe_{80}Zr_7B_{12}Cu$, respectively. ΔE_Q is the average quadrupole splitting of a-$Fe_2B_{0.625}Zr_{0.375}$ obtained from a two-line fit (right scale). B_a is the average hyperfine field and $2\Gamma_{res.am.}$ is the full linewidth of the residual amorphous phase of nc-$Fe_{80}Zr_7B_{12}Cu$, respectively. The left scale belongs to B_a^3, the right scale to $2\Gamma_{res.am.}$. The deduced Curie temperatures are marked by arrows.

On the other hand, Curie point determination of the residual amorphous phase, T_c^a, is much more complicated. It is partly due to the concentration fluctuations and due to the difficulty that the transition takes place in the stray magnetic field (1–2 T) of the adjacent ferromagnetic granules. Two approaches can be used: T_c^a may be approximated from the

low (below T_c^a) and from the high (above T_c^a) temperature range as shown in figure 3. In the low temperature approximation T_c^a is determined from the B_a^3–T plot as $T_c^a = 351 \pm 5$ K, which is analogous to the often used magnetic method [1, 4]. This T_c^a value is 45 K lower than that measured for the bulk amorphous sample. Similarly to the average hyperfine fields it can also be explained by a slightly lower Fe concentration (4 at.%, which is close to the accuracy of the bcc-Fe fraction determination). In the high temperature approach, the width of the broadened central line corresponding to the paramagnetic residual amorphous phase will significantly increase below T_c^a. This approach extrapolates to $T_c^a = 455$ K. The overestimation originates from the line broadening effects due to chemical fluctuations and the stray magnetic field of the neighbouring ferromagnetic bcc granules resulting in damping of the paramagnetic relaxation. Previous results [5] for the nanocrystallized low (below 6 at.%) B content amorphous Fe–B–Zr–Cu ribbons show only a limited excess broadening of the hyperfine field distribution and the T_c values determined from the ferromagnetic and from the paramagnetic regime gave the same value within 30 K. The larger difference is probably connected with the enhanced composition fluctuation of the present, high B content residual amorphous phase. Since in the $Fe_2(B_{1-x}Zr_x)$ amorphous series T_C changes [6] 400 K when x varies between 0.125 and 0.55, fluctuations of the B/Zr ratio can largely contribute to the smearing out of the Curie temperature.

At high temperatures, above 600 K, the line widths of the six-line components of the bcc phase show a dramatic increase (figures 4 and 5) which is reversible for temperature lowering. This phenomenon is typical of magnetic moment relaxation and is rarely observed in a broad temperature range at high temperatures because of the shortness of the Mössbauer time-window (about 10^{-8} s). The simplest possible evaluation is the determination of the temperature dependence of the line width. The line width of the main component of the bcc phase, Γ_{main}, is used because systematic errors originating from line overlap influence it to a lesser extent. $\Gamma_{main} = \Gamma_0 + \Delta\Gamma$, where Γ_0 is the average line width determined below 600 K and $\Delta\Gamma$ is the excess line broadening due to relaxation. $\Delta\Gamma$ is proportional to the inverse superparamagnetic relaxation time, τ^{-1}. It is given [15] for non-interacting particles by the Néel-Brown expression as $\tau = \tau_0 e^{\Delta E/k_B T}$. Here τ_0 is of the order of 10^{-10} s, ΔE is the energy barrier separating the two orientations of magnetization, and k_B is Boltzmann's constant. For particles with uniaxial symmetry $\Delta E = KV$, where K is the magnetic anisotropy constant and V is the volume of the particle. The slope of the linear plot of $\ln(\Delta\Gamma/\Gamma_0)$ versus T^{-1} shown in the inset of figure 5 gives $\Delta E/k_B = 9.5 \times 10^3$ K. It corresponds to $V = 2.6 \times 10^3$ nm^3, if the anisotropy constant of α-Fe, $K = 5 \times 10^4$ J m^{-3} is used. The characteristic size of the bcc particles calculated from this volume is 14 nm, surprisingly close to the $D = 10$ nm value measured by x-ray diffraction. The volumetric fraction of the ferromagnetic bcc granules is quite significant (they contain more than 50% of the iron atoms). The magnetic particle size is thus expected to be larger than D due to the magnetic agglomeration. No superparamagnetic relaxation was observed [5] in the nc-$Fe_{90}Zr_7B_2Cu$ sample as also shown in figures 4 and 5 for comparison. This is attributed to the larger grain size (∼20 nm from x-ray diffraction). Besides that, due to the large volume fraction of the bcc granules (containing about 80% of the iron atoms), the precipitates are more closely packed. In the present estimation of the magnetic particle size the assumed value of their magnetic anisotropy constant is quite uncertain.

Magnetization study of the superparamagnetic relaxation would give the volume of the magnetic particles. The only former report [16] of superparamagnetism in soft magnets crystallized from the amorphous state refers to nc-$Fe_{66}Cr_8CuNb_3Si_{13}B_9$. A combination of MS and magnetic measurements would allow a direct determination of both the magnetic anisotropy and the volume of the superparamagnetic granules; such an investigation is in progress.

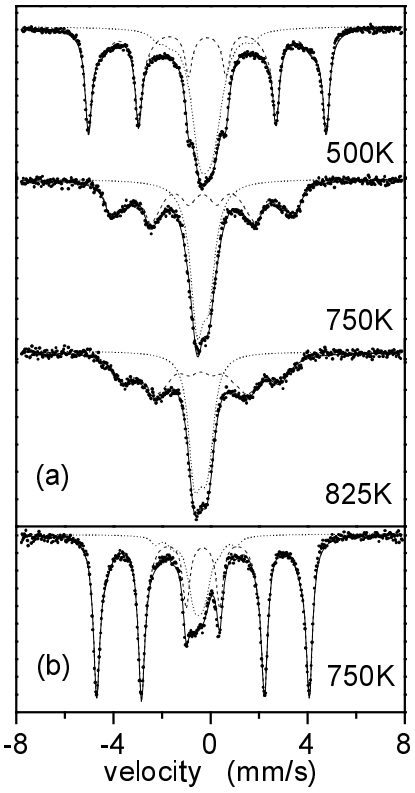

Figure 4. Typical high temperature Mössbauer spectra of nc-$Fe_{80}Zr_7B_{12}Cu$ (a) and nc-$Fe_{90}Zr_7B_2Cu$ (b), respectively. The full lines are the fitted curves, the bcc nanocrystalline component (broken line) and the residual amorphous part (dotted line) are marked.

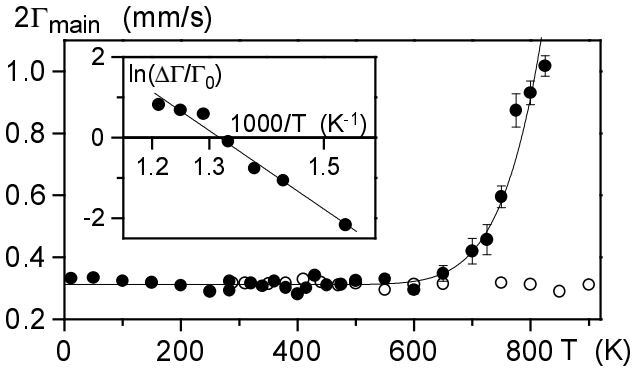

Figure 5. Temperature dependence of the full linewidth of the main bcc component for nc-$Fe_{80}Zr_7B_{12}Cu$ (full circles) and nc-$Fe_{90}Zr_7B_2Cu$ (empty circles), respectively. The inset shows the logarithm of the relative excess line broadening as the function of the inverse temperature; the full line shows a linear fit.

In conclusion, a new approach to the magnetic properties of nanocrystalline Fe–Zr–B–Cu is suggested. The role of concentration fluctuations is emphasized to explain the apparent

smearing of the Curie temperature while no Curie point enhancement is observed. The superparamagnetic relaxation of the nanosize bcc granules indicates weak magnetic coupling when the amorphous matrix is paramagnetic. The weak coupling supports some recent implications [17] that dipolar interaction is not to be neglected when the magnetic behaviours of nanoscale magnets are concerned.

Acknowledgment

This work was supported by the Hungarian Research Fund (OTKA T022413 and T020962).

References

[1] Herzer G 1993 *Nanomagnetism* ed A Hernando (Dordrecht: Kluwer) p 111
Herzer G 1995 *Scripta Met.* **33** 1741
[2] Suzuki K, Makino A, Inoue A and Masumoto T 1991 *J. Appl. Phys.* **70** 6232
[3] Hernando A and Kulik T 1994 *Phys. Rev.* B **49** 7064
Navarro I, Ortuno M and Hernando A 1996 *Phys. Rev.* B **53** 11 656
[4] Hernando A, Navarro I and Gorría P 1995 *Phys. Rev.* B **51** 3281
Hernando A, Navarro I, Prados C, García D, Vázquez M and Alonso J 1996 *Phys. Rev.* B **53** 8223
[5] Kemény T, Balogh J, Farkas I, Kaptás D, Kiss L F, Pusztai T, Tóth L and Vincze I 1998 *J. Phys.: Condens. Matter* **10** L221
Vincze I, Kemény T, Kaptás D, Kiss L F and Balogh J 1998 *Hyperfine Interact.* **113** 123
[6] Kaptás D, Kemény T, Balogh J, Bujdosó L, Kiss L F, Pusztai T and Vincze I 1999 *J. Phys.: Condens. Matter* **11** L65
[7] Orúe I, Gorría P, Plazaola M L, Fernandez-Gubieda M L and Barandiaran J M 1994 *Hyperfine Interact.* **94** 2199
[8] Navarro I, Hernando A, Vazquez M and Seong-Cho Yu 1995 *J. Magn. Magn. Mater.* **145** 313
[9] Kopcewicz M, Grabias A, Nowicki P and Williamson D L 1996 *J. Appl. Phys.* **79** 993
[10] Miglierini M and Greneche J M 1997 *J. Phys.: Condens. Matter* **9** 2303
Miglierini M and Greneche J M 1997 *J. Phys.: Condens. Matter* **9** 2321
[11] Kemény T, Varga L K, Kiss L F, Balogh J, Pusztai T, Tóth L and Vincze I 1998 *Mater. Sci. Forum* **226–229** 419
[12] Balogh J, Bujdosó L, Kemény T, Pusztai T, Tóth L and Vincze I 1997 *Appl. Phys.* A **65** 23
[13] Varga L K, Kisdi-Koszó É, Ström V and Rao K V 1996 *J. Magn. Magn. Mater.* **159** L321
Heczko O, Kraus L, Haslar V, Duhaj P and Svec P 1996 *J. Magn. Magn. Mater.* **160** 259
[14] Ayers J D, Harris V G, Sprague J A, Elam W T and Jones H N 1998 *Acta Metall. Mater.* **46** 1861
Hono K and Sakurai T 1997 *Sci. Rep. RITU* A **44** 223
[15] Hansen M F and Morup S 1998 *J. Magn. Magn. Mater.* **184** 262
[16] Slawska-Waniewska A, Gutowski M, Lachowicz H K, Kulik T and Matyja H 1992 *Phys. Rev.* B **46** 14 594
[17] Altbir D, d'Albuquerque e Castro J and Vargas P 1997 *Phys. Rev.* B **54** R6823